Supplementary Figures

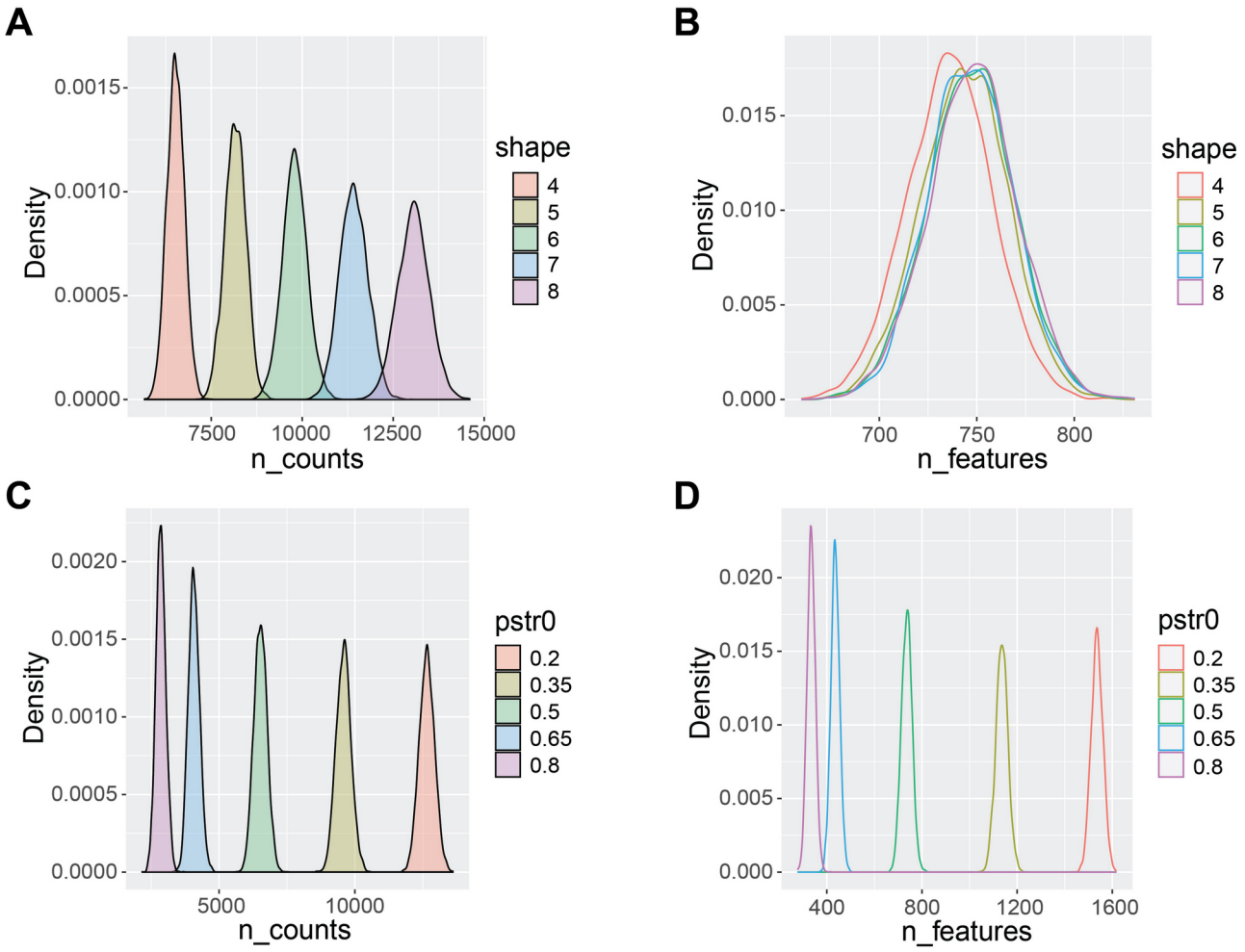

Supplementary Figure S1. Statistical characteristics of the scRNA-seq simulated datasets. (**A**) Kernel density of total numbers of counts of five simulated datasets derived from different levels of the shape parameter for the ZINB model. (**B**) Kernel density of numbers of features of five simulated datasets described in (**A**). (**C**) Kernel density of total numbers of counts of five simulated datasets derived from different levels of the pstr0 parameter for the ZINB model. (**D**) Kernel density of numbers of features of five simulated datasets described in (**C**).

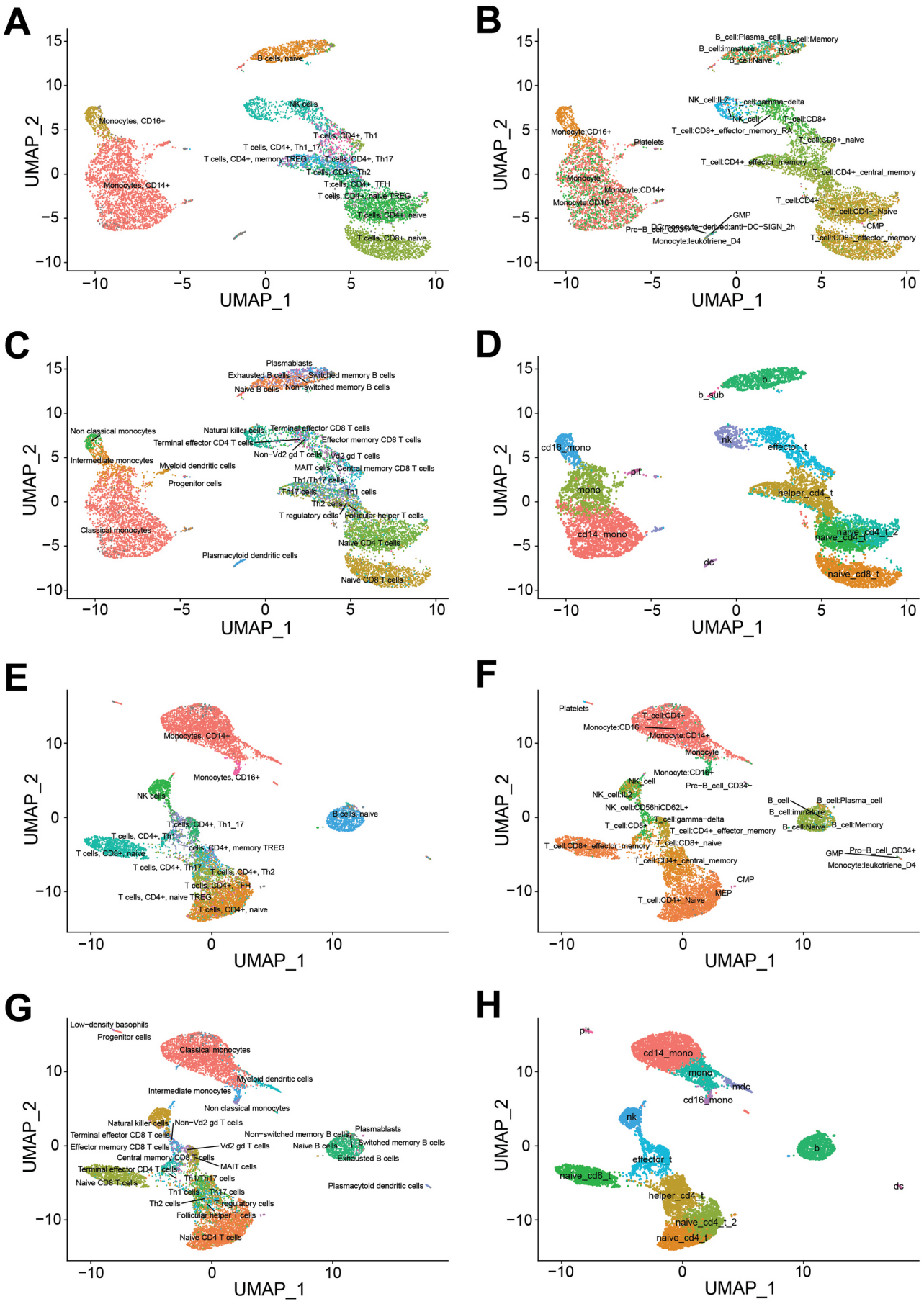
A
B
C
D
E
F
G
H
UMAP_1
UMAP_2
B cells, naive
NK cells
Monocytes, CD16+
Monocytes, CD14+
T cells, CD4+, Th1
T cells, CD4+, Th1_17
T cells, CD4+, memory TREG
T cells, CD4+, Th17
T cells, CD4+, Th2
T cells, CD4+, TFH
T cells, CD4+, naive TREG
T cells, CD4+, naive
T cells, CD8+, naive
B_cell:Plasma_cell
B_cell:Memory
B_cell:immature
B_cell
B_cell:Naive
NK_cell:IL-2
T_cell:gamma-delta
NK_cell
T_cell:CD8+
Monocyte:CD16+
T_cell:CD8+_effector_memory_RA
Platelets
T_cell:CD8+_naive
T_cell:CD4+_effector_memory
T_cell:CD4+_central_memory
Monocyte
Monocyte:CD14+
T_cell:CD4+
T_cell:CD4+_Naive
GMP
CMP
Pre-B_cell_CD34+
DC:monocyte-derived:anti-DC-SIGN_2h
Monocyte:leukotriene_D4
T_cell:CD8+_effector_memory
Plasmablasts
Exhausted B cells
Switched memory B cells
Naive B cells
Non-switched memory B cells
Non classical monocytes
Natural killer cells
Terminal effector CD8 T cells
Terminal effector CD4 T cells
Effector memory CD8 T cells
Non-Vd2 gd T cells
Vd2 gd T cells
Intermediate monocytes
Myeloid dendritic cells
MAIT cells
Central memory CD8 T cells
Progenitor cells
Th1/Th17 cells
Th17 cells
Th1 cells
Th2 cells
T regulatory cells
Follicular helper T cells
Classical monocytes
Naive CD4 T cells
Plasmacytoid dendritic cells
Naive CD8 T cells
b_stub
b
nk
cd16_mono
effector_t
plt
mono
helper_cd4_t
cd14_mono
naive_cd4_t_2
naive_cd4_t
dc
naive_cd8_t
Monocyte
Pre-B_cell_CD34+
Low-density basophils
mdc

Supplementary Figure S2. Cell identity inference of the PBMC 10k datasets. (**A-C**) Cell clusters of the PBMC 10k 3p dataset are annotated based on their similarity to the DICE (**A**), HPCA (**B**), and Monaco (**C**) reference datasets, respectively. (**D**) Manually curated cell types of the PBMC 10k 3p dataset taking into account reference data and DEGs. (**E-G**) Same as (**A-C**) but for the PBMC 10k 5p dataset. (**H**) Manually curated cell types of the PBMC 10k 5p dataset.

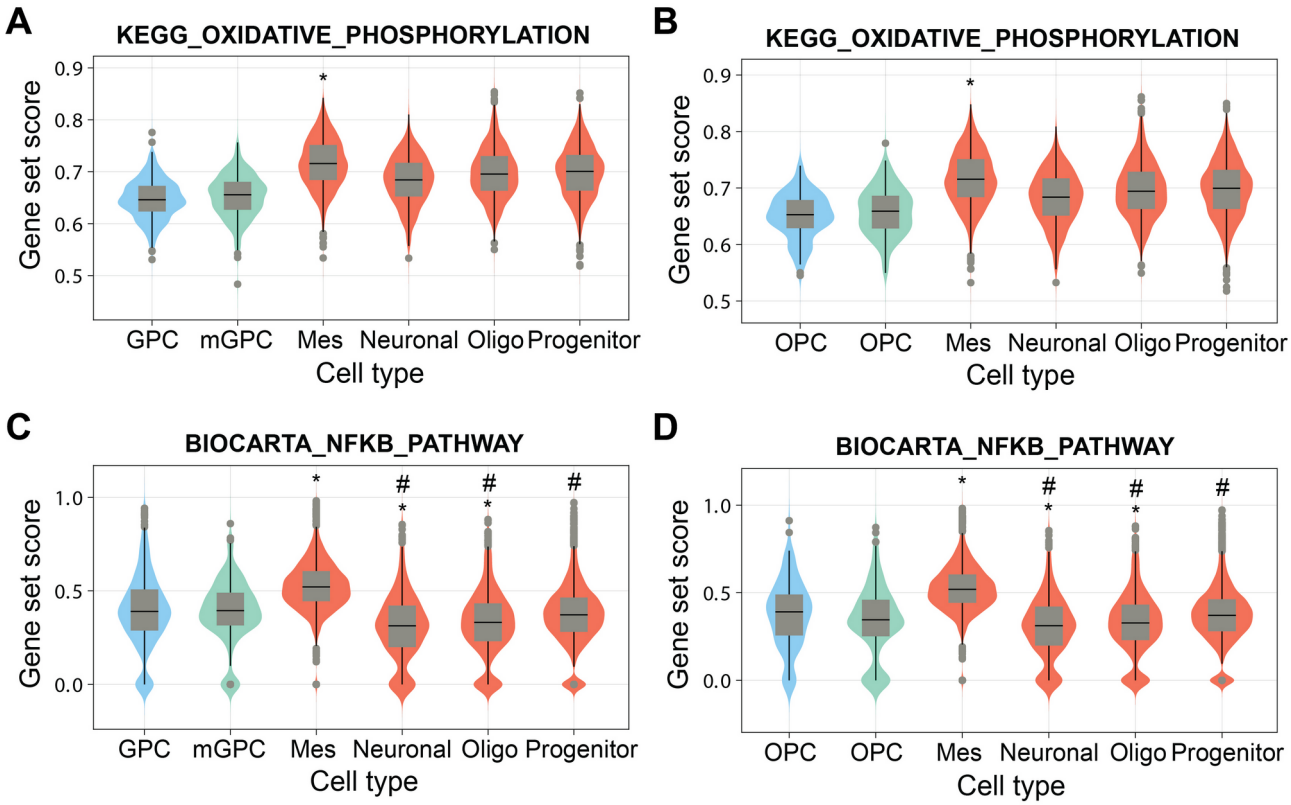

Supplementary Figure S3. Activity of oxidative phosphorylation and NF-κB pathways in glioblastoma cancer cells and cells of human fetal brain estimated by scMRGSS. (**A-B**) Gene set scores of the KEGG oxidative phosphorylation pathway in glioblastoma cancer cells when compared to GPC (**A**) and OPC (**B**) of two brain development datasets. (**C-D**) Same as (**A-B**) but for the Biocarta NF-κB pathway.